Electronic Supplementary Material (ESI) for Journal of Materials Chemistry A.

Supporting Information

Promoting Spherical Epitaxial Deposition of Solid Sulfides for High-Capacity Li-S Batteries

Kangli Xu[+], Maogen Zhu[+], Linqin Zhu, Danying Li, Wanqun Zhang, Tao Huang, Yongchun Zhu*

and Yitai Qian*

Department of Chemistry and National Laboratory for Physical Sciences at the Microscale,

University of Science and Technology of China, Hefei, Anhui, 230026, China

Corresponding authors:

ychzhu@ustc.edu.cn

ytqian@ustc.edu.cn

1. Experimental Section

CoSAs-CP electrode: $Co(NO_3)_2 \cdot 6H_2O$ (0.145g) and $Zn(NO_3)_2 \cdot 6H_2O$(0.149g) were dissolved in 20ml methanol, 2-methylimidazole (0.329g) was dissolved in another 20ml methanol. The two solutions were mixed together under stirring for 10 min at room temperature. A strip-type carbon paper was pre-treated by acetone and methanol by turns for several times. Subsequently the pretreated carbon paper was soaked in the as-prepared mixed solution, which was then treated by solvothermal at 120℃ for 5 h. The as-obtained decorated carbon paper was taken out from solution and washed with methanol several times then dried in vacuum at 60℃ for 12h. The single-atom cobalt decorated carbon paper (CoSAs-CP) was obtained by annealing the as-obtained decorated carbon paper at 800 ℃in N_2 atmosphere for 3h then cooling naturally to room temperature.

Material Characterization: Morphology information was imaged by JSM-6700F Scanning Electron Microscope (SEM) and Dimension Icon Atomic Force Microscope (AFM). X-ray Photoelectron Spectroscopy (XPS) was carried out on the ESCALAB 250 spectrometer (Perkin-Elmer) with a Kratos Analytical spectrometer and a monochromatic Al Kα (1486.6 eV) X-ray source. High-Angle Annular Dark-Field Scanning Transmission Electron Microscope (HAADF-STEM) and the corresponding Electron Energy-Loss Spectroscopy (EELS) were collected by spherical aberration corrected FEI Tecnai G2 F20 high-resolution transmission electron microscope and JEOL JEM-ARM200F TEM/STEM. Ultraviolet-Visible Spectra (UV-Vis) were acquired by the Vernier UV-VIS Spectrophotometer. X-Ray Powder Diffraction (XRD) was conducted on a Philips X' Pert Super diffractometer with Cu Kα radiation (λ=1.54178 Å).

Active material: Li_2S_8 (10 mM) was adopted as the active ingredient, which was obtained by the

chemical reaction of Li_2S and S powder with a molar ratio of 1:7 in the LiTFSI DME/DOL (1 M, v/v=1:1) solution at 70℃ for 24 h under stirring.

Electrolyte preparation: Catholyte was obtained by adding the as-prepared additive into 1 M LiTFSI in DOL/DME (v/v=1:1) with a certain proportion. For example, 20% catholyte means that contains 20% 10 mM Li_2S_8 additive and 80% LiTFSI DME/DOL (1 M, v/v=1:1) solution by percentage. Anolyte was the LiTFSI DME/DOL (1 M, v/v=1:1) solution.

Cell assembly: The Swagelok electrochemical cells were assembled in an Ar-filled glove box (H_2O, O_2 < 1 ppm). The Swagelok cell was separated into cathodic chamber and anodic chamber by LAGP ($Li_{1.5}Al_{0.5}Ge_{1.5}P_3O_{12}$, HF-Kejing) ceramic wafer. The as-prepared single-atom cobalt decorated carbon paper (CoSAs-CP) was used as working electrode in cathodic chamber containing the 100 μL catholyte. Li metal foil was used as counter electrode in anodic chamber containing the 100 μL anolyte.

Electrochemical measurements. Cyclic voltammetry (CV) was carried out on Autolab AUT302N, the scanning rate is 0.3 mV s^{-1}, and the as-obtained 40% catholyte was used as the working catholyte. Galvanostatic discharge-charge profiles were collected by LAND-CT2001A. Galvanostatic intermittent titration technique (GITT) was conducted on Autolab AUT302N, the GITT procedure was composed by 10 minutes of 50 μA galvanostatic discharge, followed by 120 minutes of relaxation, and the as-obtained 40% catholyte was used as the working catholyte. A home-made specialized electrochemical cell was used to conduct the in situ UV-Vis observation. A tailored electrochemical equipment with Al foil window was used to acquire the in situ X-ray diffraction.

Computational method: Density functional theory (DFT) calculations were performed using Vienna ab initio Simulation Package (VASP) code with the projector augmented-wave (PAW) approach[1].

Perdew-Burke-Ernzerhof generalized gradient approximation functional (GGA-PBE) was adopted to describe the electronic exchange-correlation energy[2]. All the structures were optimized within the 0.01 eV $Å^{-1}$ of the force convergence criterion by the cutoff energy of 450 eV. Static calculations were performed in supercells using *Γ*-centered 6 × 6 × 1 *k*-mesh. The binding energy (E_b) was defined as $E_b = E_{total}–E_{ads}–E_{suf}$, wherein the E_{total}, E_{ads} and E_{suf} were represented the energy of, the adsorbed system, the adsorbates and the optimized clean surface, respectively. The diffusion barriers were optimized by Climbing Image Nudged Elastic Band (CI-NEB) calculation[3] using *Γ*-centered 2 × 2 × 2 *k*-mesh.

2. Tables and Figures

Discharge product	Electron transfer(mol)	Depth of discharge (%)	Capacity (mA h g^{-1})
S_8^{2-}	0.25	12.5	209.4
S_6^{2-}	0.33	16.7	279.7
S_4^{2-}	0.5	25	418.8
S_2^{2-}	1	50	837.5
S^{2-}	2	100	1675.0

Table S1. Electron transfer and capacity contribution of cathodic reaction with depth of discharge.

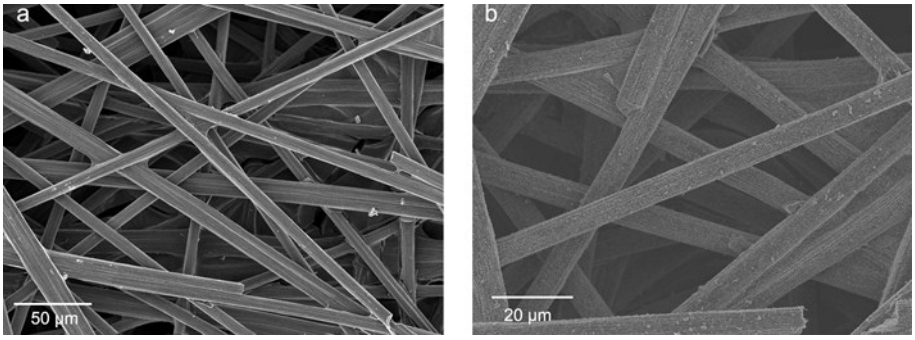

Fig. S1 SEM images of the single carbon fiber of CP (a) and of CoSAs-CP (b).

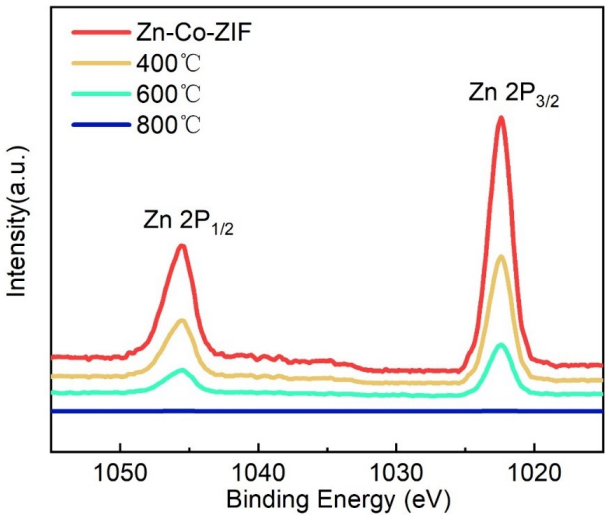

Fig. S2 The XPS spectra of Zn-Co-ZIF annealed under different temperatures.

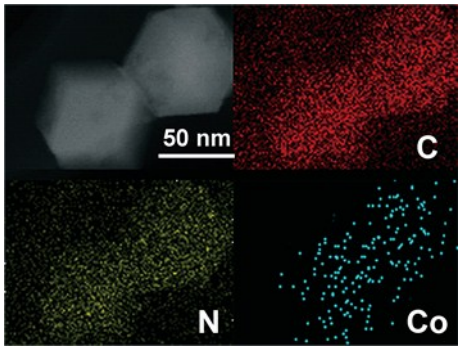

Fig. S3 Elemental spatial distribution mapping of CoSAs.

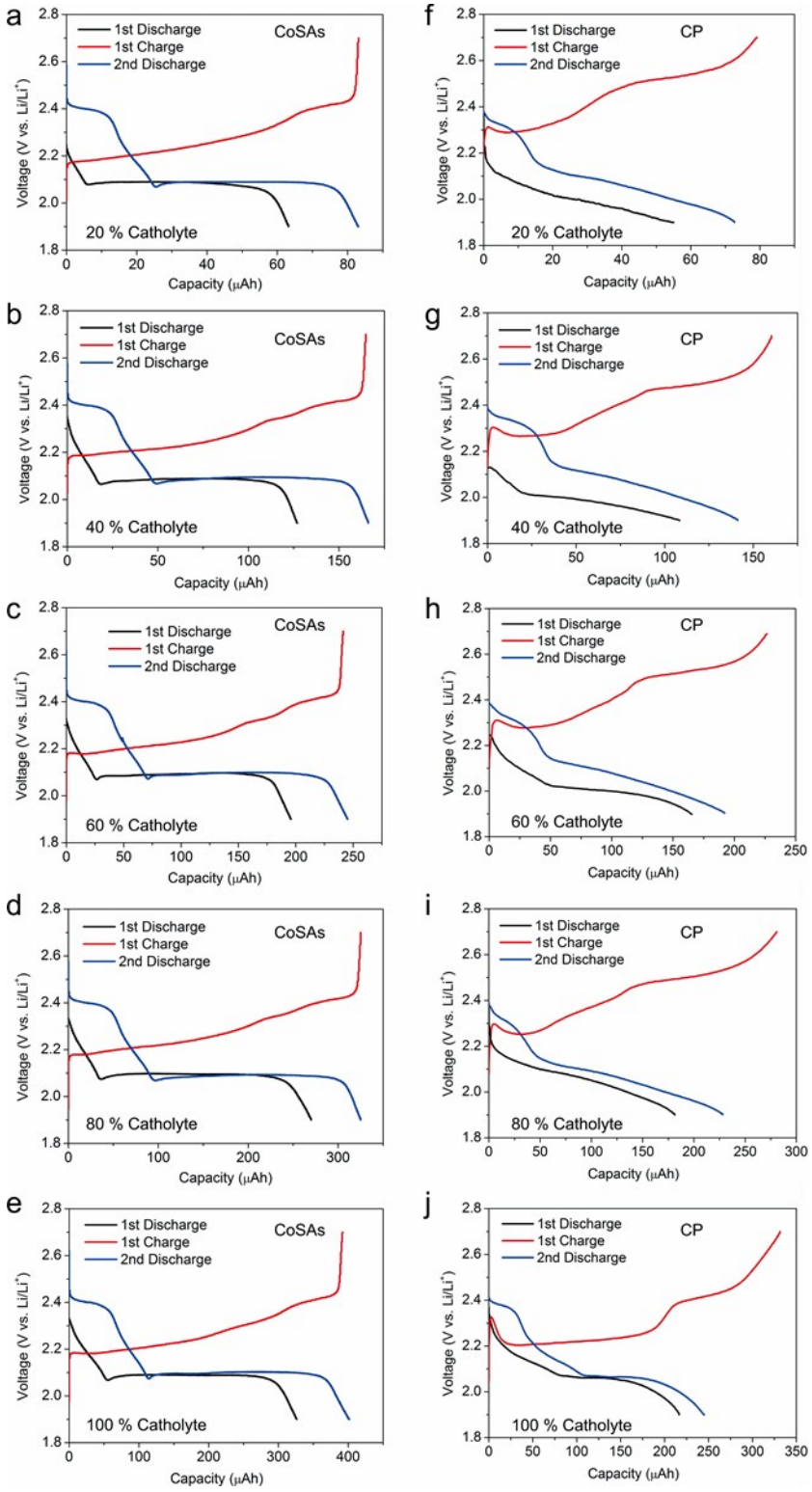

Fig. S4 PSs transformation on CoSAs-CP electrode (a-e) and CP electrode (f-j) by using different catholyte at 50 μA.

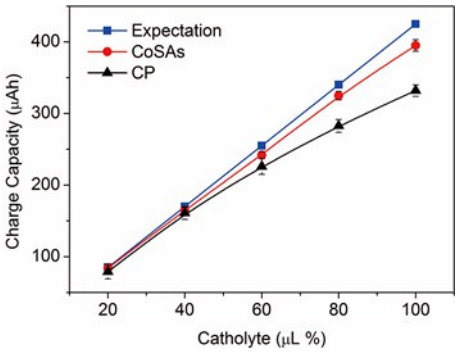

Fig. S5 Catholyte-dependence charge capacity trend.

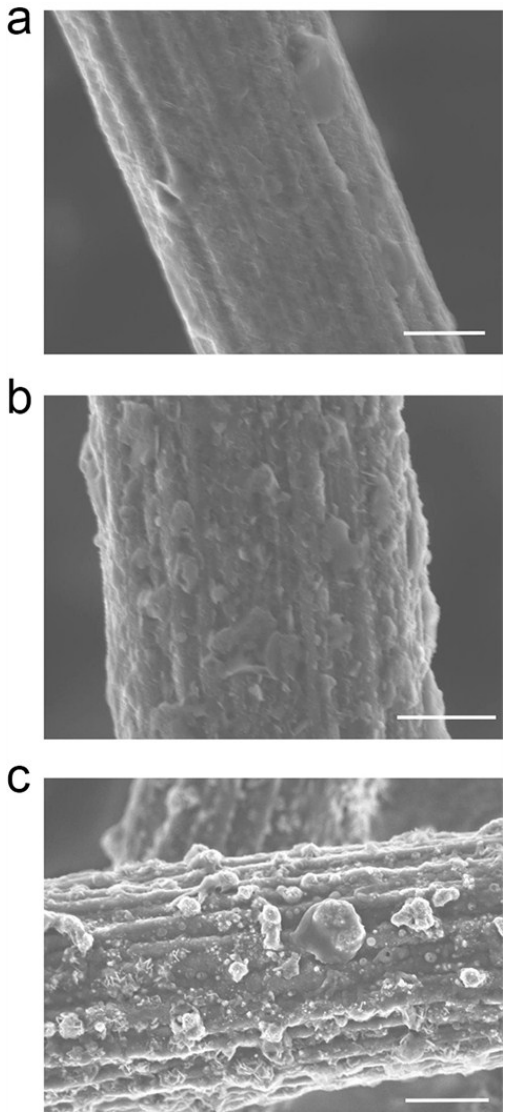

Fig. S6 The discharged N-CP electrodes using 20% (a), 60% (b) and 100% (c) catholyte. Scar bar: 2 μm.

Single-atom Co is removed from CoSAs-CP by a hydrothermal method using 1 M HCl solution at 120 ℃ for 6 h for several times until the Co cannot be tested by XPS. Then, the material without Co (N-CP) was used as the deposition substrate. Compared to the CoSAs-CP, all the morphologies of deposited N-CP were uneven. In the 20% catholyte, the deposition on the N-CP forms 2D structure obviously. In the higher concentration of catholyte, such as 60% and 100%, it shows a mixed structure containing both 2D and 3D morphology.

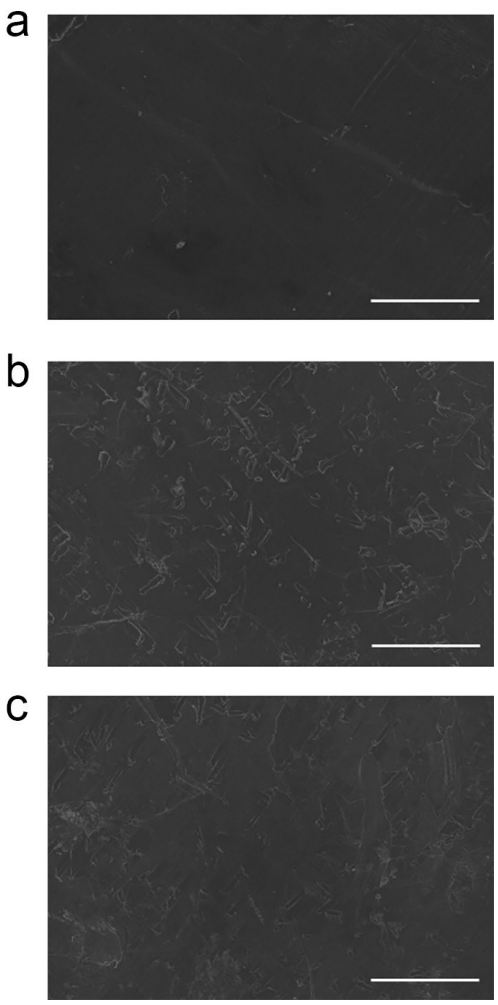

Fig. S7 a) The initial structure of Li metal anode. b) The cycled structure of Li metal anode coupled with CP. c) The cycled structure of Li metal anode coupled with CoSAs-CP. Scar bar: 20 μm.

It can be found that the cycled Li metal anodes are different from the initial one (Fig. S7a), however, the cycled Li metal anode coupled with CP (Fig. S7b) shows a similar structure with the cycled Li metal anode coupled with CoSAs-CP (Fig. S7c). This is caused by the dendrite formation of Li metal anode. This also confirms that the PSs can be confined in the cathodic chamber.

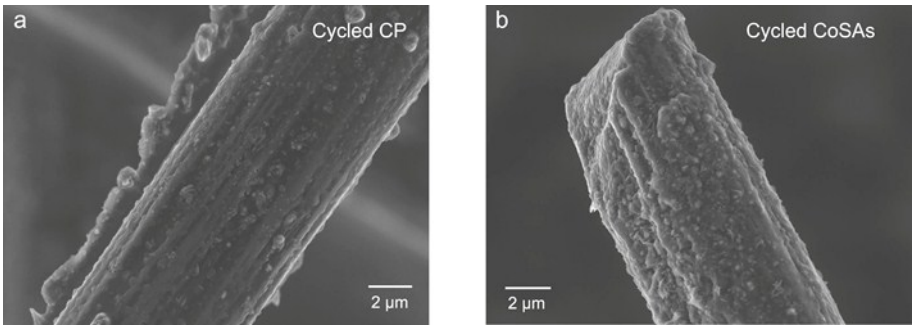

Fig. S8 SEM images of CP electrode and CoSAs-CP electrode after long cycling.

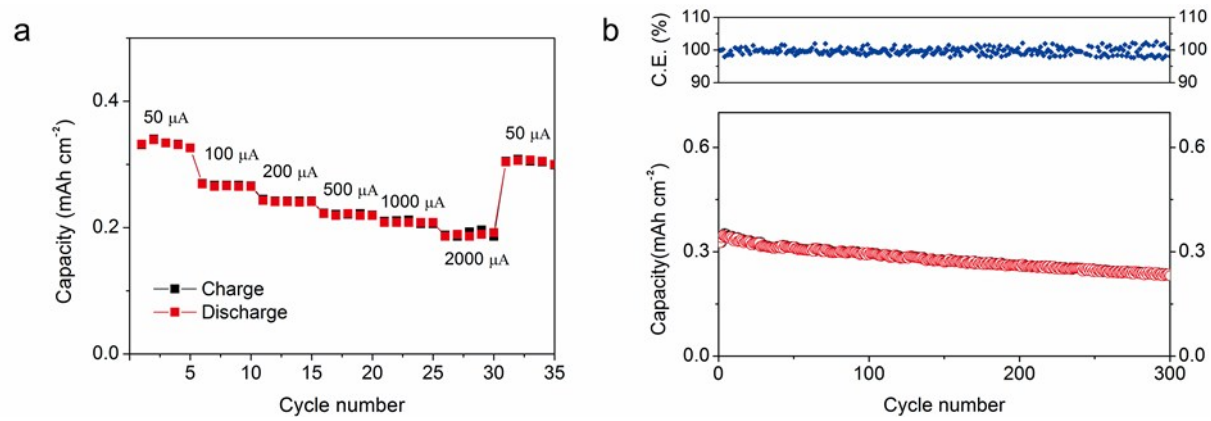

Fig. S9 (a) Rate performance of CoSAs-CP electrode with 80% catholyte. (b) Cycling performance of CoSAs-CP electrode with 80% catholyte at 50 μA.

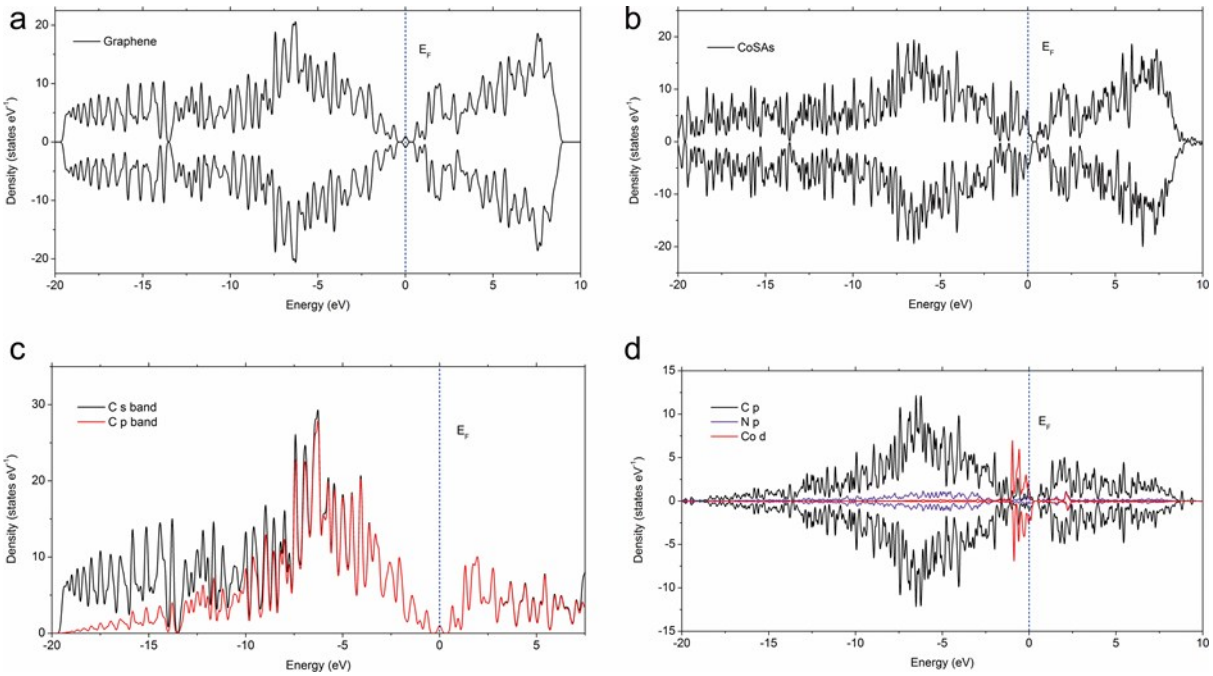

Fig S10. TDOS (a-b) and PDOS (c-d) analysis for CP (a, c) and CoSAs-CP electrode (b, d).

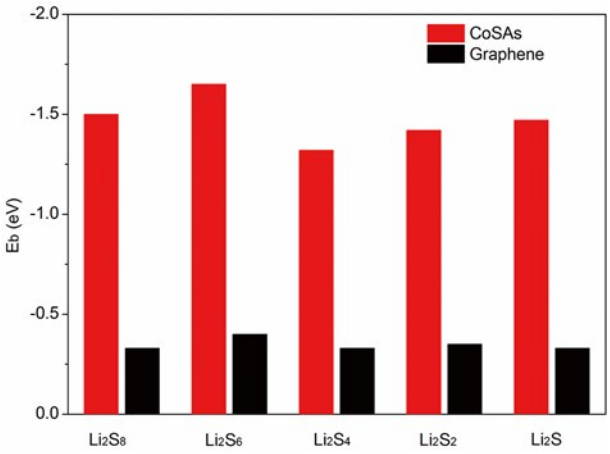

Fig. S11 Binding energy comparison for PSs species on the electrodes.

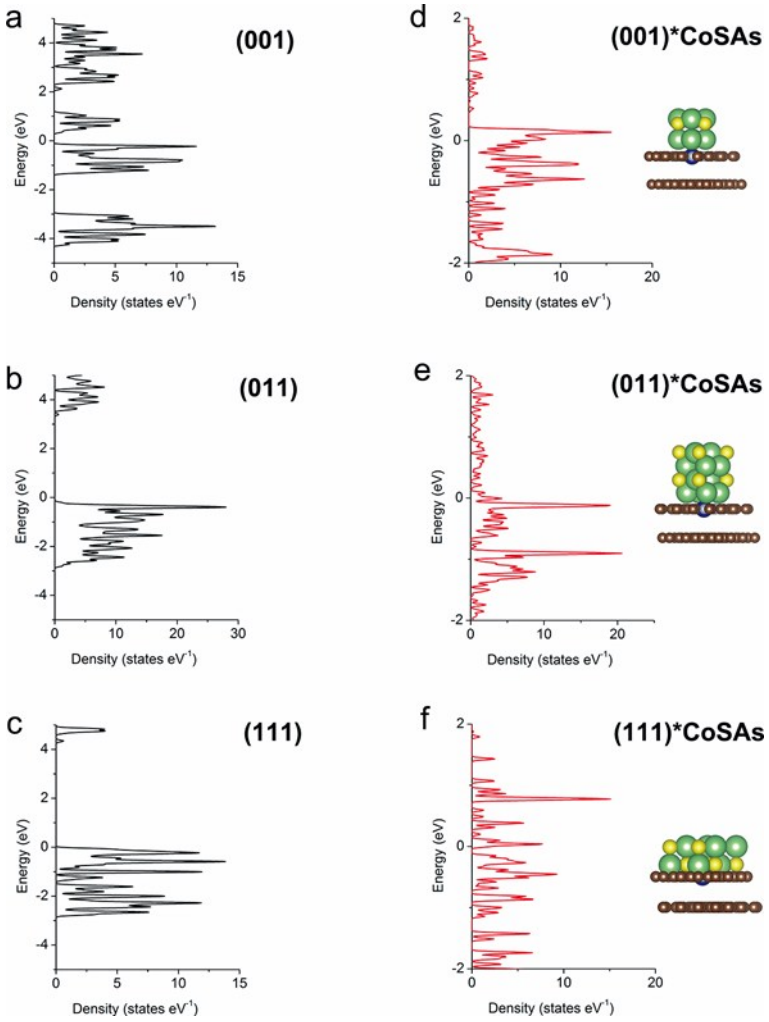

Fig. S12 TDOS of Li_2S_2 (a-c) and Li_2S_2*CoSAs (d-f).

3. Reference

1. G. Kresse and J. Furthmüller, *Phys. Rev. B*, 1996, **54**, 11169.

2. J. P. Perdew, K. Burke and M. Ernzerhof, *Phys. Rev. Lett.*, 1996, **77**, 3865.

3. G. Henkelman, B. P. Uberuaga and H. Jónsson, *J. Chem. Phys.*, 2000, **113**, 9901-9904.